Local particle flux reversal under strongly sheared flow

P. W. Terry
Department of Physics, University of Wisconsin-Madison, Madison, Wisconsin 53706

D. E. Newman
Department of Physics, University of Alaska at Fairbanks, Fairbanks, Alaska 99775

A. S. Ware
Department of Physics and Astronomy, University of Montana-Missoula, Missoula, Montana 59812

(Received 21 August 2002; accepted 16 January 2003)

The advection of electron density by turbulent **E×B** flow with linearly varying mean yields a particle flux that can reverse sign at certain locations along the direction of magnetic shear. The effect, calculated for strong flow shear, resides in the density-potential cross phase. It is produced by the interplay between the inhomogeneities of magnetic shear and flow shear, but subject to a variety of conditions and constraints. The regions of reversed flux tend to wash out if the turbulence consists of closely spaced modes of different helicities, but survive if modes of a single helicity are relatively isolated. The reversed flux becomes negligible if the electron density response is governed by electron scales while the eigenmode is governed by ion scales. The relationship of these results to experimentally observe flux reversals is discussed. © *2003 American Institute of Physics.*
[DOI: 10.1063/1.1559475]

I. INTRODUCTION

The suppression of turbulence by **E×B** flow shear has provided a compelling phenomenological paradigm for understanding transport barriers and enhanced confinement regimes in fusion plasmas.[1] However, under closer scrutiny, it is not difficult to find measurements whose details appear to be at odds with the suppression paradigm. One example is the observation in a variety of devices of fluctuation levels that change only slightly or even increase in a region of strong flow shear, but where transport is strongly suppressed.[2–7] A second example is the observation that in regions of strong flow shear, the flux can actually reverse sign and become inward. This behavior appears as a reproducible feature of probe-induced shear layers in several experiments,[6,8] and has also been observed in internally-induced shear layers in the H mode and the heliac.[9] In tokamak probe-induced shear-layers, the flux reversal occurs toward the inside edge of the shear layer, in a region of positive shear, suggesting reproducible spatial structure.[8]

A key to understanding these phenomena is the cross phase. The cross phase is the difference between phases of the two fluctuating quantities that govern fluctuation-induced transport fluxes. The behavior of the cross phase in regions of strong flow shear has only recently come under study.[10,11] This contrasts with extensive and widely pursued examinations of the effect of flow shear on fluctuation amplitudes.[1,12] Where the cross phase has been measured, however, it is observed that the cross phase can decrease in strongly sheared flow even when fluctuation amplitudes decrease only slightly, or increase. Recently, the cross phase was calculated for a generic scalar advected by a turbulent **E×B** flow with a linearly varying mean.[10] In a strong shear regime (shear rate $>$turbulent decorrelation rate), it was found that, like the experimental observations,[2–8] the cross phase decreases considerably more sharply with flow shear than does the part of the flux proportional to the absolute value of fluctuation amplitudes. While this work was based on a simple model of passive scalar transport in a uniform magnetic field, recent computational work in resistive ballooning mode turbulence shows similar behavior.[11]

The simple model of Ref. 10 yields a positive definite flux. Hence it cannot explain observations of locally reversed fluxes.[8] Nonetheless, the flux of Ref. 10 has strong spatial nonuniformity, with a narrow mixing layer whose width is proportional to the inverse of the shear strength, flanked by broad regions of strongly suppressed cross phase and transport. Given the strong spatial variations of cross phase in the simple model, we ask what additional physics could cause the cross phase to change sign. (By definition, the sign of the flux resides in the cross phase, hence flux reversals occur where the cross phase changes sign.)

In this paper, we explore the above question by introducing a second, physically distinct inhomogeneity into the process of scalar advection by inhomogeneous mean flow. A relatively simple yet pervasive inhomogeneity is that of a sheared magnetic field. The interplay of magnetic shear and uniform flow shear is known to produce oscillations in the eigenmode envelope of the dissipative trapped electron mode (DTEM).[13] The eigenmode operator of the DTEM problem is similar to the response of an electron density fluctuation whose evolution is subject to both **E×B** advection and a collisionally damped parallel flow.[14] The behavior of the DTEM eigenmode envelope, while suggestive, does not of itself guarantee flux reversal. The spatial structure of the flux is governed by a spatial integral over the inverted density response operator. To work out such details we specialize the scalar evolution of Ref. 10 to electron density and introduce magnetic shear through a collisionally damped parallel flow.

The **E×B** nonlinearity is renormalized, and the evolution operator is inverted using a Green function as in Ref. 10. Asymptotic techniques for strong shear allow for evaluation of the spatial integral and yield a fairly simple expression for the flux. The electron density-potential cross phase is found to reverse sign, independent of the eigenmode structure.

We are interested in the generic response of electron density to turbulent advection in a mean flow with linear shear and a sheared magnetic field. However, to determine whether the reversal of the cross phase carries over to a reversal in the flux, we must consider the eigenmode structure. For concreteness we examine a passing particle nonadiabatic electron response characteristic of edge conditions in the measurements cited above. It is convenient to treat the nonadiabatic electron density as the electron contribution to ion temperature gradient (ITG) turbulence. For ITG fluctuations, the adiabatic electron density, which does not contribute to transport, combines with ion dynamics to fix the radial mode structure and growth rate.[15] The nonadiabatic electron density fixes the particle transport, but makes little contribution to the mode structure and growth rate. The ITG eigenmode, which weights the cross-phase response in the flux, is centered in a region of positive flux. However, the eigenmode is displaced from the rational surface by a scale length characteristic of ion dynamics. The region of maximum density response is displaced by a scale length characteristic of electron dynamics. As a result there is very little overlap of density response and eigenmode. All contributions to the flux are highly suppressed, but the negative contributions are more suppressed than positive contributions. On the other hand, if the eigenmode structure is controlled by electron dynamics as is the case with dissipative electrons governed by the Hasegawa–Wakatani model,[16] the eigenmode and density response have significant overlap. The cross phase reverses sign on the inside edge of a shifted eigenmode, yielding a region of weak negative flux to the inside of a larger region of positive flux. This structure represents the contribution of the flux of a single helicity. If the turbulence has many helical modes whose spacing is smaller than mode widths, the negative feature is washed out in the spectrum sum. For the combination of inhomogeneities under consideration the shear must be large enough to affect electron scales.

The spatial structure of the dissipative drift wave particle flux described above and the strong shear threshold are not unlike features observed in probe-induced shear layers. However, this work suggests that where flux reversals are observed in experiment the turbulence may have a spatially localized, quasicoherent feature that avoids the washing out of regions of negative flux by neighboring mode structures. This may arise from a turbulent diffusivity that is not uniform, or from a flow that is highly localized. Describing turbulent structure in regions of nonuniform diffusivity or localized flow is a difficult problem, hence the present work is restricted to the case of uniform diffusivity and uniform flow shear. Accordingly, this work must be viewed as a plausibility study, showing that an anomalous particle flux can have radially localized regions of negative sign, and indicating the conditions that favor reversals. Beyond that, limitations in the model and calculation make comparison with experimental details premature. Subsequent theory should calculate the eigenmode structure self-consistently with the electron density response. Moreover, other more potent, but difficult-to-handle, inhomogeneities should be considered. These include the inhomogeneity of the grad-B and curvature drifts that figure in the eigenmode of toroidal ITG turbulence, and the strong variation of the shear in the highly localized flows of probe-induced transport barrier experiments. The strong variation of flow shear in highly localized flows may localize eigenmodes and isolate single helicities, or organize the flux so that contributions from differing helicities produce a negative flux in the same region.

This paper is organized as follows. In Sec. II the basic model is presented and the electron density evolution equation is inverted to obtain the flux as the product of the fluctuation magnitudes and an explicit expression for the cross phase. In Sec. III the cross phase expression is analyzed for zero crossings and plotted as a function of radius. This is the principal result of the paper. To anticipate the complete flux structure, including the eigenmode structure, the assumed behavior of an ITG eigenmode is discussed. Implications of these results for measured fluxes and future theory are discussed in Sec. IV.

II. MODEL AND CALCULATION

The electron particle flux is governed by the correlation of the electron density fluctuation $\tilde{n}$ with the fluctuation of the advecting flow. For radial transport by a turbulent **E×B** flow the flux is

$$\begin{aligned}\Gamma &= -\mathrm{Re}\langle \tilde{n} c B_0^{-1} \nabla \phi \times \mathbf{z}\cdot\mathbf{x}\rangle \\ &= \mathrm{Re}\sum_{k,\omega} i c B_0^{-1} k_y \tilde{n}_{\mathbf{k},\omega}(x)\phi_{-\mathbf{k},-\omega}(x) \\ &= -\sum_{k,\omega} c B_0^{-1} k_y |\tilde{n}_{\mathbf{k},\omega}||\phi_{-\mathbf{k},-\omega}|\sin\delta_{\mathbf{k},\omega}, \end{aligned} \tag{1}$$

where the brackets indicate an average over slab coordinates y and z, ω is the Fourier frequency and $\mathbf{k}$ is the wave vector of those directions, and $-cB_0^{-1}\nabla\phi\times\mathbf{z}$ is the fluctuating **E×B** flow expressed in terms of the electrostatic potential ϕ. The factor $|\tilde{n}_{\mathbf{k},\omega}||\phi_{-\mathbf{k},-\omega}|$ represents the amplitude dependence of the flux. The last equality defines the cross phase $\delta_{\mathbf{k},\omega}$ as the difference between phases of the scalar and the electrostatic potential fluctuation. The coherence, which generally appears as an additional factor in the last expression, is assumed to be unity.

To describe the electron density fluctuation we consider a collisional regime consistent with ion temperature gradient turbulence with a collisional nonadiabatic electron density response.[14] The electron density satisfies a continuity equation subject to a fluctuating collisional flow along the magnetic field and the perpendicular **E×B** flow with mean and fluctuating components. The parallel electron flow is governed by

$$n_e m_e \frac{dv_\parallel}{dt} + \nabla_\parallel p_e = e n_e \nabla_\parallel \phi - n_e m_e \nu_{ei} v_\parallel, \tag{2}$$

where ν_{ei} is the electron–ion collision rate and other symbols have their usual meaning. For isothermal electrons and weak electron inertia the parallel flow fluctuation is $v_\parallel = -(T_e/n_0 m_e \nu_{ei})\nabla_\parallel \tilde{n} - (e/m_e \nu_{ei})\nabla_\parallel \phi$, where n_0 and T_e are the equilibrium electron density and temperature. With this expression for parallel flow the electron continuity equation is

$$\frac{\partial \tilde{n}}{dt} - \frac{V_e^2 n_0}{\nu_{ei}} \nabla_\parallel^2 \left(\frac{e\phi}{T_e} - \frac{\tilde{n}}{n_0} \right) + v_0(x) \frac{\partial \tilde{n}}{\partial y} - \frac{c}{B_0} \nabla \phi \times z \cdot \nabla \tilde{n} = \frac{c}{B_0} \nabla \phi \times z \cdot \nabla n_0(x), \tag{3}$$

where the mean **E×B** flow $v_0(x)$ is a poloidal flow with radial shear, and V_e is the electron thermal velocity. Introducing the nonadiabatic electron density, $h_e = \tilde{n}/n_0 - e\phi/T_e$, the evolution equation for h_e is given by

$$\frac{\partial h_e}{\partial t} - \frac{V_e^2}{\nu_{ei}} \nabla_\parallel^2 h_e + v_0(x) \frac{\partial h_e}{\partial y} - \frac{c}{B_0} \nabla \phi \times z \cdot \nabla h_e = -\left(\frac{\partial}{\partial t} + v_0(x) \frac{\partial}{\partial y} \right) \frac{e\phi}{T_e} + \frac{c}{n_0 B_0} \nabla \phi \times z \cdot \nabla n_0(x). \tag{4}$$

The mean flow is assumed to have a linear variation, $v_0(x) = v_0(x_R) + (x - x_R) v_0'$, where x_R is the position of a rational surface. Hereafter x will indicate the distance from the rational surface, i.e., $x - x_R \to x$. We introduce a Fourier transform for both time and the y direction. Note that in general, the flow does not vanish at the rational surface. However, the Doppler shift from this uniform flow component, $k_y v_0(x_R)$ is adsorbed into the frequency ω, i.e., $\omega - i k_y v_0(x_R) \to \omega$. The turbulent frequency spectrum $|\phi_{\mathbf{k},\omega}|^2$ typically develops the same Doppler shift. This means that when the sum over frequency in the flux expression is carried out, the Doppler shift frequency dependence in the electron response [inversion of the left-hand side of Eq. (4)] is evaluated at the Doppler shifted peak of the frequency spectrum. As a result, the Doppler shift cancels out, and Eq. (1) becomes $\Sigma_{\mathbf{k}} c B_0^{-1} k_y |\tilde{n}_{\mathbf{k},\omega}| |\phi_{-\mathbf{k}}| \sin \delta_{\mathbf{k},\omega_p}$, where $\omega_p = \omega_r(k) + i\omega_i(k)$, $\omega_r(k)$ is the peak of the frequency spectrum for wave number k *in the plasma frame*, $\omega_i(k)$ is the width of the spectrum, and $|\phi_{\mathbf{k}}|^2$ is the magnitude of the frequency spectrum at its peak value. A sheared slab is assumed for the magnetic field, with the usual result that under the Fourier transform, $\nabla_\parallel^2 \to -k_y^2 x^2 / L_s^2$, where L_s is the magnetic shear scale length.

The Fourier transform of Eq. (4) is

$$-i(\omega - k_y v_0' x) h_{\mathbf{k},\omega}(x) + \frac{V_e^2 k_y^2 x^2}{\nu_{ei} L_s^2} h_{\mathbf{k},\omega}(x) + \sum_{\mathbf{k}',\omega'} \frac{c}{B_0} \Big[-i k_y' \phi_{\mathbf{k}',\omega'} \frac{\partial}{\partial x} h_{\mathbf{k}-\mathbf{k}',\omega-\omega'} + i(k_y - k_y') h_{\mathbf{k}-\mathbf{k}',\omega-\omega'} \frac{\partial}{\partial x} \phi_{\mathbf{k}',\omega'} \Big] = i(\omega - k_y v_0' x - \omega_*) \frac{e\phi_{\mathbf{k},\omega}}{T_e}, \tag{5}$$

where $\omega_* = -(cT_e/eB_0) k_y n_0^{-1} dn_0/dx$ is the diamagnetic frequency. We renormalize Eq. (5) using the eddy damped quasinormal Markovian closure, adapted to the inhomogeneous nonlinearity. Details are given in Refs. 13 and 17. Under this procedure the nonlinearity is expressed as an amplitude-dependent diffusion and a nonlinear (amplitude-dependent) damping rate. The resulting equation is

$$-i(\omega - k_y v_0' x) h_{\mathbf{k},\omega}(x) + \frac{V_e^2 k_y^2 x^2}{\nu_{ei} L_s^2} h_{\mathbf{k},\omega}(x) - \frac{\partial}{\partial x} D_{\mathbf{k},\omega} \frac{\partial}{\partial x} h_{\mathbf{k},\omega}(x) + k_y^2 d_{\mathbf{k},\omega} h_{\mathbf{k},\omega}(x) = i(\omega - k_y v_0' x - \omega_*) \frac{e\phi_{\mathbf{k},\omega}}{T_e}, \tag{6}$$

where the turbulent diffusivities $D_{\mathbf{k},\omega}$ and $d_{\mathbf{k},\omega}$ are given by

$$D_{\mathbf{k},\omega} = \sum_{\mathbf{k}',\omega'} \frac{c^2}{B_0^2} k_y' (k_y' - k_y) \phi_{\mathbf{k}',\omega'}(x) R_{\mathbf{k}'',\omega''} \phi_{-\mathbf{k}',-\omega'}(x),$$

$$d_{\mathbf{k},\omega} = \sum_{\mathbf{k}',\omega'} \frac{c^2 (k_y' - k_y)}{B_0^2 k_y} \frac{\partial \phi_{\mathbf{k}',\omega'}}{\partial x} R_{\mathbf{k}'',\omega''} \frac{\partial \phi_{-\mathbf{k}',-\omega'}}{\partial x}, \tag{7}$$

and $R_{\mathbf{k}'',\omega''}$ is the nonlinear response at wave number $k'' \equiv k - k'$ and frequency $\omega'' \equiv \omega - \omega'$:

$$R_{\mathbf{k}'',\omega''} = \left[-i\omega'' + i k_y'' x v_0' + \frac{V_e^2 k_y''^2 x^2}{\nu_{ei} L_s^2} - \frac{\partial}{\partial x} D_{\mathbf{k}'',\omega''} \frac{\partial}{\partial x} - (k_y - k_y')^2 d_{\mathbf{k}'',\omega''} \right]^{-1}. \tag{8}$$

Note that the response at k'', ω'' has been expanded about the rational surface for the mode k, ω.

Our objective is to invert Eq. (6) to obtain the spatial structure of $h_{\mathbf{k},\omega}(x)$ consistent with the source on the right-hand side and the spatial characteristics of the operator on the left-hand side. Note that the EDQNM closure yields a diffusivity that is nonuniform, with spatial variation arising both from the potential ϕ and the operator of the nonlinear response, Eq. (8). Given this nonuniformity, inversion of Eq. (6) is highly nontrivial. If the fluctuation spectrum has modes at different locations in x (corresponding to different rational surfaces), such that the separation between adjacent modes is smaller than the spatial extent of individual modes, then the nonuniformity in the components of D gets smoothed by the sum over wave number. This situation is common when there is magnetic shear, making the approximation of uniform D a standard approximation. Even if D is not uniform, the wave number sum tends to make D smoother than h or R. In the asymptotic limit of strong shear, this leads to singular layer structure in h, with the nonuniformity of D a higher order variation. The diffusivity can be treated as uniform in determining leading order behavior. These arguments do not preclude the possibility of a diffusivity with strong variation under certain circumstances. For example, near low order rational surfaces the distance between rational surfaces with significant fluctuation activity can exceed the fluctuation widths. In the vicinity of the low order surface the sum over

wave number does little smoothing. This situation has been studied in a limited fashion with the result that turbulence levels are essentially impervious to flow shear.[13] Because the effect on the particle flux was not determined, this is an interesting area for future investigation.

We proceed with the inversion of Eq. (6) for the case in which the turbulent diffusivity is smooth. The inversion is accomplished with a Green function,

$$h_{\mathbf{k},\omega}(z)=\int dx' \times G(x|x')\frac{i(\omega-k_y v_0' x'-\omega_*)}{D_{\mathbf{k},\omega}}\frac{e\phi_{\mathbf{k},\omega}(x')}{T_e} \tag{9}$$

where the Green function $G(x|x')$ satisfies

$$\frac{d^2}{dx^2}G(x|x')-Q(x)G(x|x')=-\delta(x-x'), \tag{10}$$

and

$$Q(x)=\frac{1}{\Delta^4}\left[\left(x-\frac{iS\Delta}{2}\right)^2-\Delta^2\lambda\right], \tag{11}$$

is an effective potential obtained by completing the square on the magnetic and flow shear inhomogeneities of the density evolution, and

$$\lambda=-\left[\frac{S^2}{4}-iS\left(\frac{\omega}{\omega_s}+\frac{ik_y^2 d_{\mathbf{k},\omega}}{\omega_s}\right)\right]$$

is an effective eigenvalue. The potential and Green function have a nominal, no-flow width Δ, whose form

$$\Delta=\left(\frac{D_{\mathbf{k},\omega}\nu_{ei}L_s^2}{V_e^2k_y^2}\right)^{1/4}, \tag{12}$$

is typical for an electron response in the presence of damped parallel electron flow. The potential is shifted by $S\Delta/2$ along the imaginary x axis, where S is the BDT shear strength,[18]

$$S=\frac{k_y v_0'\Delta}{D_{\mathbf{k},\omega}/\Delta^2}, \tag{13}$$

representing the ratio of the **E×B** shearing rate, $\omega_s=k_y v_0'\Delta$, to the turbulent decorrelation rate D/Δ^2.

The Green function can be obtained from exact solutions of the homogeneous equation $d^2y/dx^2-Qy=0$, using either Hermite polynomials as eigenmodes of the homogeneous equation, or parabolic cylinder functions. The former gives the expansion

$$G(x|x')=\Delta\sum_{n=0}^{\infty}(2n+\lambda)^{-1} \times\exp\left[\frac{-(x+iS\Delta/2)^2}{2\Delta^2}\right]\exp\left[\frac{-(x'-iS\Delta^*/2)^2}{2\Delta^{*2}}\right] \times H_n\left(\frac{x+iS\Delta/2}{\Delta}\right)H_n\left(\frac{x'-iS\Delta^*/2}{\Delta^*}\right), \tag{14}$$

while the latter gives a closed-form representation,

$$G(x|x')=\frac{\Delta}{2}\frac{\hat{\Gamma}(1/2-\lambda/2)}{\pi^{1/2}}U\left(\frac{-\lambda}{2},\frac{x_>+iS\Delta/2}{\Delta/\sqrt{2}}\right) \times U\left(\frac{-\lambda}{2},-\frac{x_<+iS\Delta/2}{\Delta/\sqrt{2}}\right), \tag{15}$$

where U is the parabolic cylinder function,[19] $\hat{\Gamma}$ is the gamma function, and $x_>$ ($x_<$) is the larger (smaller) of x and x'. In terms of either of these expressions the flux is given by

$$\Gamma=-\mathrm{Re}\sum_{k,\omega}cB_0^{-1}k_y\phi_{-\mathbf{k},-\omega}(x)n_0\int_{-\infty}^{\infty}dx'G(x|x') \times\frac{(\omega-k_y v_0' x'-\omega_*)}{D_{\mathbf{k},\omega}}\frac{e\phi_{\mathbf{k},\omega}(x')}{T_e}. \tag{16}$$

Neither Eq. (14) or (15) allow the integral in Eq. (16) to be evaluated in terms of an analytic expression using tabulated or simple functions. Therefore, we turn to asymptotic methods to infer basic scalings. The relevant limit for significant suppression of transport is the limit of strong shear, or the asymptotic limit $S\to\infty$. However, even in this limit, it is not possible to evaluate the integral in Eq. (16) using Eq. (14) or (15), because the appropriate asymptotic expansions are not readily available in the reference literature. To proceed we return to Eq. (10) and solve it approximately using asymptotic methods.

In the asymptotic limit of strong shear, $Q\to\infty$. Hence asymptotic solutions for the homogeneous equation are obtained using WKB theory. From these solutions an asymptotic expansion of the Green function is constructed by matching across the singularity, yielding

$$G(x|x')\sim\frac{\Delta^2}{2g'\left(\frac{x'+iS\Delta/2}{\Delta}\right)f\left(\frac{x'+iS\Delta/2}{\Delta}\right)} \times f\left(\frac{x+iS\Delta/2}{\Delta}\right) \times\exp\left[-g\left(\frac{x_>+iS\Delta/2}{\Delta}\right)\right] \times\exp\left[+g\left(\frac{x_<+iS\Delta/2}{\Delta}\right)\right], \quad (S\to\infty), \tag{17}$$

where $g'(y)=dg/dy$, and

$$g(y)=\frac{y}{2}(y^2-\lambda)^{1/2}, \tag{18}$$

$$f(y)=(y^2-\lambda)^{-1/4}[y^2+(y^2-\lambda)^{1/2}]^{-\lambda/2}. \tag{19}$$

With the asymptotic Green function of Eq. (17) substituted into Eq. (16), the integral can be evaluated using Laplace's method. The exponential functions in $G(x|x')$ carry a factor $S^{3/2}$, making the exponentials vary more rapidly in the limit of large shear than any other function in $G(x')$ or the flux integral of Eq. (16). For large S the exponentials produce a boundary layer at $x'=x$ that dominates the flux integral and allows integration via Laplace's method. The resulting expression for the leading order asymptotic flux in the limit of large shear is

$$\Gamma \sim -\mathrm{Re}\sum_{\mathbf{k},\omega} \frac{cT_e}{eB_0}\frac{n_0 k_y}{2}\left|\frac{e\phi_{\mathbf{k},\omega}(x)}{T_e}\right|^2\left[\frac{\omega-\omega_*}{D_{\mathbf{k},\omega}/\Delta^2}-S\frac{x}{\Delta}\right] \times \frac{\left\{\left[\frac{x^2}{\Delta^2}+\frac{iSx}{\Delta}-iS\left(\frac{\omega}{\omega_s}+\frac{ik_y^2 d_{\mathbf{k},\omega}}{\omega_s}\right)\right]\left[\frac{x^2}{\Delta^2}-\frac{iSx}{\Delta}-\frac{S^2}{8}+\frac{iS}{2}\left(\frac{\omega}{\omega_s}-\frac{ik_y^2 d_{\mathbf{k},\omega}}{\omega_s}\right)\right]^2\right\}}{\left|\left[\frac{x^2}{\Delta^2}+\frac{iSx}{\Delta}-\frac{S^2}{8}-\frac{iS}{2}\left(\frac{\omega}{\omega_s}+\frac{ik_y^2 d_{\mathbf{k},\omega}}{\omega_s}\right)\right]^2\right|^2}, \quad (S\to\infty). \tag{20}$$

The flux has spatial structure arising from the eigenmode envelope $|\phi_{\mathbf{k},\omega}(x)|^2$, and the remaining x-dependent terms, which originate with the density response $\tilde{n}_{\mathbf{k},\omega}(x)/\phi_{\mathrm{k},\omega}(x)$. These two sources of spatial variation are separated in Eq. (20). This result does not require that the eigenmode have smoother variation than the remaining terms in Eq. (20), which represent the integrated density response. Rather, it requires the limit of large shear. If S is not sufficiently large, higher order terms in the asymptotic expansion of the integral might be required for accuracy. These bring in derivatives of the eigenmode and hence sample eigenmode variation in the integral of Eq. (16).

The cross phase and the possibility of flux reversals reside in the density response, because the eigenmode envelope is positive definite. The spatial structure of the density response is considerably more complicated than it is for the case in which the only homogeneity arose from the mean flow.[10] The structure is in large measure nonlinear, and is not captured by the quasilinear approximation. For comparison the quasilinear flux is

$$\Gamma \sim -\mathrm{Re}\sum_{k,\omega} \frac{cT_e}{eB_0}\frac{n_0 k_y}{2}\left|\frac{e\phi_{\mathbf{k},\omega}(x)}{T_e}\right|^2 \times\left[\frac{\omega-\omega_*}{\omega}-S\frac{x}{\delta}\right]\left[1-s\frac{x}{\delta}+i\frac{x^2}{\delta^2}\right]^{-1}, \tag{21}$$

where $\delta^2=(\omega\nu_{ei}L_s^2/V_e^2k_y^2)$ and $s=k_yV_0'\delta/\omega$.

The eigenmode envelope is also the spectrum of the electrostatic potential. We will model the frequency spectrum as a Lorentzian that peaks at a value $\omega=\omega_r(k)$ and has a width $\omega_i(k)$. The frequency of the peak is the linear mode frequency shifted by the Doppler frequency of the flow at x_R and a nonlinear frequency.[20] The width arises from the incoherent drive of fluctuations by mode coupling, and is related to $\mathrm{Re}\,D_{\mathbf{k},\omega}$ and $\mathrm{Re}\,d_{\mathbf{k},\omega}$. With the frequency spectrum so modeled, the sum over ω in Eq. (21) can be carried out. The flux is unchanged from Eq. (20), provided the sum is understood to be over $\mathbf{k}$ only, $\phi_{\mathbf{k},\omega}(x)$ is replaced by $\phi_{\mathbf{k}}(x)$, the amplitude of the Lorentzian, and ω in the remainder of the expression is understood to be $\omega_r(k)+i\omega_i(k)$.

III. CROSS PHASE CHARACTERISTICS

The flux given in Eq. (20) is well behaved for real values of x; zeros of the denominator are all complex. The flux is positive asymptotically as $x\to\infty$. If the flux reverses sign, the factors in the numerator of the density response must pass through zero for a real value of x. While the density response factor can be evaluated numerically and figures showing the numerical evaluation appear below, it is useful to obtain analytical approximations for the zeros, as these will provide the basis for scaling relations. We therefore examine the zeros of the seventh order polynomial that constitutes the real part of the numerator of the density response,

$$\mathrm{Re}\left\{\left[S\frac{x}{\Delta}-\frac{\omega-\omega_*}{D_{\mathbf{k},\omega}/\Delta^2}\right]\left[\frac{x^2}{\Delta^2}+\frac{iSx}{\Delta}-iS\left(\frac{\omega}{\omega_s}+\frac{ik_y^2 d_{\mathbf{k},\omega}}{\omega_s}\right)\right] \times\left[\frac{x^2}{\Delta^2}-\frac{iSx}{\Delta}-\frac{S^2}{8}+\frac{iS}{2}\left(\frac{\omega}{\omega_s}-\frac{ik_y^2 d_{\mathbf{k},\omega}}{\omega_s}\right)\right]^2\right\}=0. \tag{22}$$

It is often true that $\mathrm{Re}\,D_{\mathbf{k},\omega}\gg\mathrm{Im}\,D_{\mathrm{k},\omega}$. We will simplify the analysis of Eq. (22) by assuming that $D_{\mathbf{k},\omega}$ (and hence Δ) is real.

Equation (22) is not factored because we must take the real part of complex factors. The seventh order polynomial with real coefficients that results from this operation is complicated but zeros can be found approximately by assuming $S\gg1$ and using asymptotic analysis. We expand the zeros as an asymptotic series in S, $x=\Delta(x^{(0)}+S^{-1}x^{(1)}+S^{-2}x^{(2)}+\cdots)$, and look first for zeros with $x^{(0)}\sim\mathrm{O}(1)$. The lowest order balance is

$$Sx^{(0)}\left[-15(x^{(0)})^2S^4+\frac{3}{2}S^5\left(\frac{\omega_i(k)-k_y^2\,\mathrm{Re}\;d_{\mathbf{k},\omega}}{\omega_s}\right)\right]=0, \tag{23}$$

where we recall that $\omega_s=SD_{\mathbf{k},\omega}/\Delta^2$ implies that $\omega_s=\mathrm{O}(S)$. There are three order-unity zeros:

$$x\sim0, \quad \pm\Delta\frac{1}{\sqrt{10}}\left(\frac{\omega_i(k)-k_y^2\,\mathrm{Re}\,d_{\mathbf{k},\omega}}{\omega_s/S}\right)^{1/2}, \quad (S\to\infty). \tag{24}$$

The frequency spectrum linewidth typically represents a nonlinear damping process, making $\omega_i(k)<0$. If $d_{\mathbf{k},\omega}$ acts as a saturation mechanism. $\mathrm{Re}\,d_{\mathbf{k},\omega}>0$. In this case, the two zeros from the quadratic factor form a complex conjugate pair, and the only order-unity zero for real x is $x=0$. The remaining zeros are singular, i.e., they scale as S to a positive power. We assume $x^{(0)}\sim\mathrm{O}(S)$ and find a lowest order balance given by

$$Sx^{(0)}[(x^{(0)})^6+\tfrac{3}{4}S^2(x^{(0)})^4-\tfrac{15}{16}S^4(x^{(0)})^2]=0. \tag{25}$$

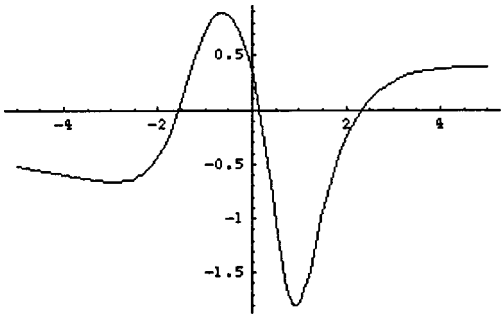

FIG. 1. Full density response for $S=3$, $\omega_r/\omega_s=0.3$, $\omega_i/\omega_s=-0.3$, and $\omega_*/\omega_s=0.1$.

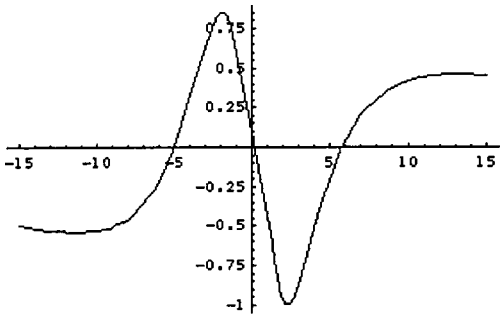

FIG. 3. Full density response for $S=10$, $\omega_r/\omega_s=0.3$, $\omega_i/\omega_s=-0.3$, and $\omega_*/\omega_s=0.1$.

The three roots with $x^{(0)}=0$ correspond to the order-unity roots of Eq. (24). The remaining four roots satisfy $(x^{(0)})^2=S^2(-3\pm\sqrt{24})/8$. From the upper branch there are two real zeros,

$$x=\pm\Delta S\left(\frac{\sqrt{24}-3}{8}\right)^{1/2}\approx\pm\frac{\Delta}{2}S \tag{26}$$

and from the lower branch there is a complex conjugate pair,

$$x=\pm i\Delta S\left(\frac{\sqrt{24}+3}{8}\right)^{1/2}. \tag{27}$$

Under this arrangement of three real zeros, the density response is positive for $x\gtrsim\Delta s/2$ and negative for $0<x\lesssim\Delta s/2$. For negative values of x the flux is first positive between 0 and $-\Delta s/2$, and then negative for $-x\gtrsim-\Delta s/2$. The full density response [the negative of everything to the right of $|e\phi_{\mathbf{k}}(x)/T_e|^2$ in Eq. (20)] is plotted in Figs. 1–4 for different values of S and ω_i/ω_r. (Recall that the density response is only one component of a Fourier sum over $\mathbf{k}$.) Figures 1–3 represent parameters typical of ITG turbulence and Fig. 4 is typical of drift wave turbulence. The three real zeros are clearly evident, as is their basic scaling with S. The structure of positive and negative regions described above is also evident. The magnitude of the minimum and maximum inside the region of the outermost zeros ($|x|\approx\Delta s/2$) are somewhat larger than those for $|x|\gtrsim\Delta s/2$. The density response is strongly suppressed by flow shear in the central region. Taking $x\sim0$ and substituting into the density response, we find that it goes roughly as S^{-4}. On the other hand, the outer maximum and minimum, which peak near $x=\Delta S$, are essentially unaffected by flow shear. Taking $x=\Delta S$ and substituting into the density response, we find that it is of order unity in this region. This behavior is also evident in the figures, which shows the central minimum becoming less deep as S increases, while the rightmost maxima is unchanged in magnitude.

This absence of scaling with the shear parameter in the outer lobes contrasts with the case where inhomogeneity resides solely in the flow.[10] There, transport is unimpeded by flow shear only in a Kelvin mixing layer whose width decreases as shear increases. Everywhere else transport is strongly suppressed. The difference can be traced directly to the advection of potential, $v_0(x)\partial\phi/\partial y$, in the source of the nonadiabatic density. This term makes the source of the nonadiabatic density go as $Sx/\Delta\sim S^2$, canceling a factor S^{-2} from the inversion of the density response operator. In Ref. 10, the flux was calculated directly from the full density $\tilde{n}$. There was no factor $v_0(x)\partial\phi/\partial y$ in the source of the density, and the inverse S-scaling of the operator inversion governed the response for large x. If the flux is calculated from the full density $\tilde{n}$ as in Ref. 10, we obtain the same result as obtained with the nonadiabatic density. However, the additional S^2 scaling arising originally from the source of the nonadiabatic density has its origin in the inhomogeneity of the magnetic shear damping. This inhomogeneity, and that of the flow, are in balance precisely at $x=S\Delta$. Calculating the transport from the density $\tilde{n}$, the magnetic shear damping term proportional to the potential [second term of Eq. (3)] now enters the density source as a term proportional to x^2. At $x=S\Delta$ this term is equal to the advective factor in the nonadiabatic source, yielding the same flux. We conclude that the interaction of the inhomogeneity of magnetic shear damping and a *linear*

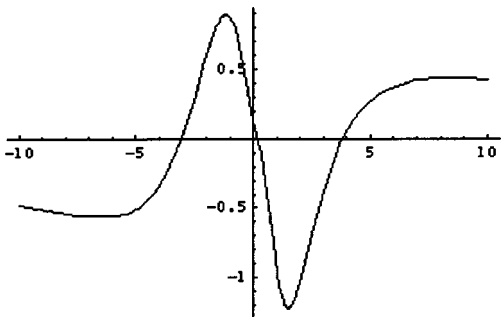

FIG. 2. Full density response for $S=6$, $\omega_r/\omega_s=0.3$, $\omega_i/\omega_s=-0.3$, and $\omega_*/\omega_s=0.1$.

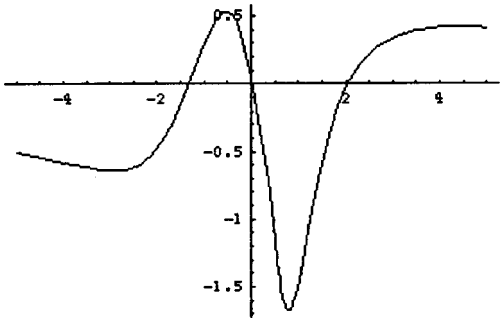

FIG. 4. Full density response for $S=3$, $\omega_r/\omega_s=0.3$, $\omega_i/\omega_s=-0.1$, and $\omega_*/\omega_s=0.3$.

flow shear inhomogeneity produces a fundamental displacement $x=S\Delta$ (where the frequencies of the two processes balance), at which the density response has a local maximum and is independent of S. This is an outcome of the linear flow shear profile, and shows that the cross phase is sensitive to the flow profile. This matter is discussed further in Sec. IV.

We now consider the eigenmode envelope $|\phi_{\mathbf{k}}(x)|^2$, which weights the density response. The eigenmode envelope is also affected by the interplay of quadratic and linear inhomogeneities of magnetic shear damping and flow shear. However, the eigenmode potential is typically more complicated than $Q(x)$, the effective potential of the density response [Eq. (11)]. We will consider two types of eigenmodes, one whose scales are governed by ion dynamics, and one whose scales are governed by electron dynamics. For the former we have in mind the eigenmode of the fluid ITG instability in a sheared slab; for the latter, we consider dissipative drift waves as modeled by the Hasegawa–Wakatani equation. Both situations have complicated eigenmode problems whose solution and details are beyond the scope of the present theory, which emphasizes the nonlinear electron response. However, the ITG eigenmode in the presence of strong flow shear has been studied,[21] and we perform a simple analysis to make a crude estimate of the scales associated with features of the numerically evaluated eigenmode. For the Hasegawa–Wakatani eigenmode we simply note the scale of the magnetic shear damping, and contrast the situation to that of the ITG mode.

In simple models, like that of dissipative tapped electron mode turbulence,[13] the balance of the linear flow shear inhomogeneity and the quadratic magnetic shear damping inhomogeneity unequivocally determines the shift of the eigenmode away from the mode rational surface. The eigenmode of ITG turbulence is considerably more complicated, but also has a shift that increases with flow shear strength.[21] The eigenmode is governed by ion equations for vorticity, pressure, and parallel flow, and adiabatic electronic according to $d^2\phi/dx^2+P(x)\phi=0$, where

$$P(x)=-k_y^2\rho_s^2+\frac{1-\overline{\omega}}{\overline{\omega}+(1+\eta_i)\tau}+\frac{(L_n/L_s)^2x^2/\rho_s^2}{\overline{\omega}^2-(\gamma/\tau)(L_n/L_s)^2x^2}, \tag{28}$$

$\overline{\omega}=[\omega+k_y v_0' x]/\omega_*$, γ is the ratio of specific heats, and $\tau=T_e/T_i$. We note that for $v_0'\to\infty$, the potential P becomes independent of x. Consequently the shift cannot be found by simply taking the balance of the shear damping term and the other flow shear-dependent term in the limit of strong shear. However, if we assume that the numerator of the second term is dominated by the flow shear, while the frequencies in the denominators are dominated by the growth rate $\omega_*(1+\eta_i)\tau$, the balance of these terms yields a shift that is proportional to the flow shear,

$$x_{\mathrm{ITG}}=\rho_s^2\left(\frac{k_y v_0'}{\omega_*}\right)(1+\eta_i)\tau\left(\frac{L_s}{L_n}\right)^2. \tag{29}$$

The precise form of this shift or its scalings will not be particularly important for the conclusions that follow. What will be is the fact that its overall scale is set by ion dynamics. Evaluating the flux at this spatial position,

$$\begin{aligned}\Gamma\sim&-\sum_{\mathbf{k}}\frac{cT_e}{eB_0}n_0k_y\left|\frac{e\phi_{\mathbf{k}}(x_{\mathrm{ITG}})}{T_e}\right|^2k_y^2\rho_s^2\left(\frac{\Delta}{\Delta_{\mathrm{ITG}}}\right)^4\\&\times\frac{1}{(1+\eta_i)\tau(L_s/L_n)}\\=&-\sum_{\mathbf{k}}\frac{cT_e}{eB_0}n_0k_y\left|\frac{e\phi_{\mathbf{k}}(x_{\mathrm{ITG}})}{T_e}\right|^2k_y^2\rho_s^2\frac{\omega_*\nu_{ei}L_n^2}{V_e^2(1+\eta_i)\tau},\end{aligned} \tag{30}$$

where $\Delta_{\mathrm{ITG}}=\rho_s(L_s/L_n)^{1/2}(1+\eta_i)^{1/2}\tau^{1/2}$ is a nominal zero flow-ITG linear mode width obtained using $\omega\approx\omega_*(1+\eta_i)\tau$. The zero-flow flux is

$$\begin{aligned}\Gamma&=\Sigma(cT_e/eB_0)n_0k_y|e\phi/T_e|^2(\omega_i/\omega_r)\\&\approx\Sigma(cT_e/eB_0)n_0k_y|e\phi/T_e|^2.\end{aligned}$$

Hence the factors to the right of $|e\phi/T_e|^2$ in Eq. (30) are reduction factors in the electron response, or cross phase. For TEXTOR parameters,[3] the reduction factor is $O(10^{-7})$. The precise number is unimportant, given the crudeness of the approximations used in obtaining Eq. (7). However, it is clear that where there is a flow-shear-induced shift of the eigenmode set by ion scales and a flow-shear-induced shift of the electron density response set by electron scales, the large difference in these scales yields a very small overlap of functions, and a correspondingly large reduction in the flux. The reduction is independent of shear because $x_{\mathrm{ITG}}\sim v_0'$, as discussed above. The reduction is so large that the flux is reduced below the levels of collision-driven fluxes, making the oscillations of the electron density response inconsequential.

We now consider the eigenmode of the Hasegawa–Wakatani model. The eigenmode structure is governed by electron dynamics. The magnetic shear inhomogeneity is $(V_e^2n_0/\nu_{ei})\nabla_\parallel^2$ in both the electron density equation and the equation that governs the electrostatic potential. Consequently scales are set by the electron parallel flow damping, both in the eigenmode envelope and the electron density response. There are no unequal shifts set by the disparate scales of ion and electron dynamics. We anticipate that the sign changes of the electron density response can emerge from the weighting by the eigenmode envelope. If the eigenmode is shifted by $x=S\Delta$, the eigenmode preferentially weights the positive lobe of the density response at the same location. The negative lobe between $x=S\Delta/2$ and $x=0$ contributes to the flux but with weaker weighting. Because the eigenmode shift is to the right of the rational surface, the density response structure to the left of the rational surface overlaps with the eigenmode tail, and therefore has very small magnitude. Details require a full eigenmode analysis, which will be undertaken in future work.

We have essentially been looking at a single wave number $\mathbf{k}$. The flux sums over wave number components of $|\phi_{\mathbf{k}}|^2$. In a system with magnetic shear the eigenfunctions whose wave numbers represent different helicities are centered at different radial locations. If the linear flow shear variation extends over many rational surfaces, the eigenmode of each helicity has a similar shape. The sum then represents a sum of fluxes with similar spatial structure, one for each

helicity, each displaced by the distance between rational surfaces. For shifted eigenmodes governed by electron scales, the smaller negative flux contribution between $0<x<S\Delta$ on rational surface will be destroyed by positive flux contributions of other helicities provided the separation between rational surfaces is smaller than the width of the single helicity flux structure, $x_{R2}-x_{R1}\lesssim\Delta$. Negative flux contributions can survive when this condition is violated, but in such a case that the diffusivity also starts to become nonuniform. It is more likely that the flux reversals observed experimentally are associated with a localized region of strong shear. If a localized region of strong shear affects substantially a single rational surface, the eigenmode and density response on that surface will be shifted away from the other unshifted eigenmodes with little overlap from differing helicities. Again, the diffusivity may be nonuniform in such a case. In the case of a nonuniform diffusivity the eigenmode structure can be modified in such a way as to defeat flow-shear-induced stabilization.[13] Because the shear-induced dephasing of the transport cross phase is a different process, it is likely that the cross phase and transport are reduced even though there is little change in fluctuation level.

IV. CONCLUSIONS AND IMPLICATIONS

This study was motivated by observations of localized regions of reversed particle flux in several experiments.[6,8,9] Because fluxes are typically thought of as being either uniformly outward, or uniformly inward, we have sought to determine if a locally reversed flux is possible under a simple combination of inhomogeneities. If the only inhomogeneity is that of uniform shear flow, the flux is uniformly outward. If, however, a quadratically varying inhomogeneity from magnetic shear is included, a locally reversed flux is possible, subject to certain conditions and caveats. Locally reversed flux is not likely to be observable in ITG turbulence, due to the wide separation of electron response and eigenmode functions. It can occur in fluctuations with a single scale, such as collisional drift waves, provided the spectrum is dominated by a narrow range of helicities. Such a quasi-coherent fluctuation spectrum may be favored by biased probes, whose extremely strong flow shear may significantly alter eigenmode structures and the fluctuation spectrum. In addition to answering the direct question of whether a locally reversed flux is possible for a simple combination of inhomogeneities, this work carries a variety of implications.

With a second inhomogeneity in the system, the cross phase and transport are sensitive to the shape of the flow profile. The shape of the profile potentially affects the spatial structure of the flux, the width of the mixing layer, and shear strength scalings. For the system considered here, the linearly varying $\mathbf{E}\times\mathbf{B}$ shearing rate and the quadratically varying magnetic shear damping rate are in balance at a displacement $x=S\Delta$ from the rational surface. This causes the shear-induced reduction of the density response function to be canceled by a matching increase in the density source. As a consequence, at precisely the point where the density response is maximum, it is independent of the shearing rate S. Moreover, the width of the mixing layer goes like $\Delta x=S\Delta$. These effects arise from the interplay linear and quadratic inhomogeneities. If the only inhomogeneity of the system comes from the flow, the mixing layer width goes like $\Delta x\sim S^{-1}$.[10] In both cases the flow is the same. These differences in shear scaling are due to the presence of the additional inhomogeneity of the magnetic field. The apparent universal nature of transport suppression by $\mathbf{E}\times\mathbf{B}$ flow shear applies only to homogeneous turbulence. In this regard transport suppression is similar to the turbulent structure function, whose scaling symmetries are broken by inhomogeneity in turbulence. This means that in the presence of inhomogeneity, a property intrinsic to confined plasmas, the behavior of transport in the presence of flow is sensitive to the flow profile. If the turbulence is inhomogeneous on the scale of the flow variation, a low order Taylor-series expansion of the flow (e.g., to include only the linear or quadratic variation) is insufficient to determine general transport behavior. This is true for the cross phase, as illustrated by the comparison of the results of Ref. 10 with those of the present study, but is also true for turbulent amplitudes.

A locally reversed flux obviously has implications for the particle balance and density profile evolution. Absent a specification of sources and sinks, the present calculation, which yields a flux with nonzero gradient, implies that the mean density must evolve. Because the calculation assumes a fixed gradient, the calculated flux is therefore instantaneous, and subject to change on the transport time scale as the density evolves. A locally inward flux tends to flatten the density profile, eventually stopping transport in that region. However, the experiments with observed flux reversals are presumably not in a relaxed steady state. To make complete sense of them requires a knowledge of sources, sinks, collisional fluxes, and possible poloidal asymmetry, all of which lie outside the scope of the present treatment. For example, the reversed anomalous particle flux in CHS is exceeded in magnitude by the neoclassical flux, yielding a net outward flux.[6] The inward flux observation in TEXTOR,[8] assuming it characterizes stationary transport, and assuming that the anomalous flux is larger than the neoclassical flux, suggests the need to check experimentally for poloidal asymmetry, or to consider the possibility of some self-regulatory process of source structure.

Fluxes that proceed up the gradient must not violate thermodynamic constraints, which apply to diagonal transport terms in the transport matrix. (The particle flux driven by the density gradient is a diagonal term.) For ITG turbulence, a particle flux up the gradient is possible because it is driven by free energy in the ion temperature gradient, an off-diagonal process. The only requirement is that the electron contribution to the growth rate must be small.[15] For collisional drift wave fluctuations, particle transport is driven by the density gradient. Consequently a uniformly inward flux is possible only if the growth rate is negative. (For example, collisional drift wave fluctuations, stabilized by the electron temperature gradient, would drive a transient flux up the gradient while they are decaying from some initial finite-amplitude level.) For a localized flux reversal, the thermodynamic constraint is less stringent. Because the growth rate can be related to a radial integral over the particle flux, a

locally inward flux is possible, provided the radially integrated flux is outward. This situation seems to be almost guaranteed from the uniform shear flow considered here. The shear flow shifts the eigenmode to the rightmost region of positive flux, thus giving weaker weighting to the negative flux region.

We have shown that the density response at a given wave number reverses sign in a strong shearing regime. This does not automatically guarantee that the flux reverses sign, because contributions from other wave numbers may wash out the reversal. A consideration of the sum over wave numbers raises numerous complications, which may affect the flux in situations like those of experiments where local flux reversals are observed. If the fluctuation structure has a sufficiently strong single helicity component for the reversed flux structure of the helicity to avoid being washed out by positive flux contributions from other helicities, it becomes much less likely that the assumption of a smooth diffusivity remains valid. Having a smooth diffusivity was crucial for the approximations made in this paper. Moreover, under a spectrum with a strong single helicity component, it is not likely that the eigenmode structure can be treated independently of the electron response as it was for ITG. It also appears likely that conditions that favor narrow helicity bands and flux reversals may require a shearing region that is strongly localized, not one that extends to arbitrarily large displacements. In such cases it appears important that theoretical analyses utilize experimentally realistic flow profiles over their entire extent. While detailed observations of localized flux reversals have come mostly from probe induced shear layers, it is probably true that localized flow profiles and nonuniform diffusivities may better typify conditions attendant to the H mode than the linear profiles and uniform diffusivities that have been the staple of analysis. The complications enumerated in this paragraph generally have not been considered in calculating nonlinear fluxes and the cross phase, and represent the direction in which future theoretical work should move.

ACKNOWLEDGMENTS

Helpful discussions with J. Boedo are acknowledged.

This work was supported by the US Department of Energy under Grant No. DE-FG02-89ER-53291.

[1] P. W. Terry, Rev. Mod. Phys. **72**, 109 (2000).
[2] R. A. Moyer, K. H. Burrell, T. N. Carlstrom *et al.*, Phys. Plasmas **2**, 2397 (1995).
[3] J. Boedo, P. W. Terry, D. Gray, R. S. Ivanov, R. W. Conn, S. Jachmich, G. Van Oost, and the TEXTOR Team, Phys. Rev. Lett. **84**, 2630 (2000).
[4] V. Antoni, E. Martines, D. Desideri, L. Fattorini, G. Serianni, M. Spolaore, L. Tramontin, and N. Vianello, Plasma Phys. Controlled Fusion **42**, 83 (2000).
[5] J. S. Sarff, A. F. Almagri, J. K. Anderson *et al.*, Czech. J. Phys. **50**, 1471 (2000).
[6] M. G. Shats, K. Toi, K. Ohkuni *et al.*, Phys. Rev. Lett. **84**, 6042 (2000).
[7] G. Tynan, L. Schmitz, R. W. Conn, R. Doerner, and R. Lehmer, Phys. Rev. Lett. **68**, 3032 (1992).
[8] J. Boedo, D. Gray, P. W. Terry, S. Jachmich, G. R. Tynan, R. W. Conn, and the TEXTOR-94 Team, Nucl. Fusion **42**, 117 (2002).
[9] M. G. Shats and D. L. Rudakov, Phys. Rev. Lett. **79**, 2690 (1997).
[10] P. W. Terry, D. E. Newman, and A. S. Ware, Phys. Rev. Lett. **87**, 185001 (2001).
[11] G. F. Figarella, S. Benkadda, P. Beyer, X. Garbet, and I. Voitsekhovitch, Phys. Rev. Lett. (to be published).
[12] K. H. Burrell, Phys. Plasmas **4**, 1499 (1997).
[13] B. A. Carreras, K. Sidikman, P. H. Diamond, P. W. Terry, and L. Garcia, Phys. Fluids B **4**, 3115 (1992).
[14] P. W. Terry and P. H. Diamond, Phys. Fluids **28**, 1419 (1985).
[15] B. Coppi and C. Spight, Phys. Rev. Lett. **41**, 551 (1978); P. W. Terry, Phys. Fluids B **1**, 1932 (1989).
[16] A. Hasegawa and M. Wakatani, Phys. Rev. Lett. **50**, 682 (1983).
[17] P. W. Terry, D. E. Newman, and N. Mattor, Phys. Fluids A **4**, 927 (1992).
[18] H. Biglari, P. H. Diamond, and P. W. Terry, Phys. Fluids B **2**, 1 (1990).
[19] M. Abramowitz and I. A. Stegun, *Handbook of Mathematical Functions* (Dover, New York, 1972).
[20] N. Mattor and P. W. Terry, Phys. Fluids B **4**, 1126 (1992).
[21] X.-H. Wang, P. H. Diamond, and M. N. Rosenbluth, Phys. Fluids B **4**, 2402 (1992).